Mechanistic Studies of the Hydroformylation of 1-Alkenes Using a Monodentate Phosphorus Diamide Ligand

Saskia C. van der Slot,† Paul C. J. Kamer,† Piet W. N. M. van Leeuwen,*,† Jonathan A. Iggo,‡ and Brian T. Heaton‡

Institute of Molecular Chemistry, University of Amsterdam, Nieuwe Achtergracht 166, 1018 WV Amsterdam, The Netherlands, and Department of Chemistry, Donnan and Robert Robinson Laboratories, University of Liverpool, P.O. Box 147, Liverpool, U.K. L69 7ZD

Received September 13, 2000

The mechanism of the rhodium-catalyzed hydroformylation reaction using a monodentate phosphorus diamide ligand has been investigated. The system presents an ideal case to illustrate the basics of hydroformylation. A detailed kinetic study and (in situ) spectroscopic techniques revealed that several of the elementary reaction steps are involved in the hydroformylation rate control. Which step is rate-determining depends strongly on the conditions used. Deuterioformylation showed that alkene coordination followed by hydride migration is irreversible under the conditions studied. The rhodium hydride complex $HRhL_2(CO)_2$ and several rhodium−acyl complexes were observed during the hydroformylation reaction. The structures of the rhodium−acyl complexes have been characterized using ^{31}P, ^{13}C, and ^{103}-Rh NMR spectroscopy. The major rhodium−acyl complex formed, $RC(O)RhL_2(CO)_2$, has a trigonal-bipyramidal structure with the two phosphorus ligands coordinated in the equatorial plane. The exchange rates of the equatorial and apical carbonyl ligands with dissolved carbon monoxide differ significantly, the equatorial carbon monoxide being much more labile.

Introduction

Rhodium-catalyzed hydroformylation has been extensively studied.[1−8] An important aspect of these studies has been the unraveling of the reaction mechanism in order to obtain a better understanding of the outcome of the overall reaction. Although the reaction kinetics have been investigated many times, very little has been reported on the characterization of the intermediates present during the reaction. Nowadays high-pressure (HP) spectroscopic techniques are regularly applied to identify organometallic compounds present under high pressures.[3,8−11] HP IR is most often applied to identify in situ hydroformylation intermediates, but only information about carbonyl ligands has been obtained and full characterization has not been achieved. HP NMR spectroscopy is a powerful technique for the characterization of complexes formed under high pressures. However, in situ characterization of complexes present during catalysis cannot be performed using an HP NMR tube because of diffusion limitation of the reacting gases. A continuous supply of gas and optimal mixing is achieved in an HP NMR flow cell,[12] and therefore, this is an elegant tool for the characterization of hydroformylation reaction intermediates. The combination of (in situ) HP IR and HP NMR spectroscopy can lead to complete structural analysis of the intermediates present during catalysis.

The generally accepted, dissociative mechanism proposed by Wilkinson[13] is presented in Scheme 1. The five-coordinate rhodium bisphosphine complexes shown in this scheme can be resting states of the catalyst, but rhodium complexes with one or three phosphine ligands may also be involved.[1,6,8] The reactive species in this mechanism are coordinatively unsaturated complexes formed by dissociation of CO or phosphine. A free coordination site for alkene coordination is obtained in the CO dissociation step of the rhodium hydride complex **2a** (steps 1 and 2). After hydride migration (step 3) and coordination of CO, insertion of CO occurs to give a rhodium−acyl complex (**2g**, steps 4 and 5). The unsaturated rhodium−acyl complex **2g** undergoes either hydrogenolysis (step 6) or CO coordination (step 7). Hydrogenolysis completes the catalytic cycle with the

* To whom correspondence should be addressed. E-mail: pwnm@anorg.chem.uva.nl.
† University of Amsterdam.
‡ University of Liverpool.

(1) Osborn, J. A.; Wilkinson, G.; Young, J. F. *Chem. Commun.* **1965**, 17.
(2) Brown, J. M.; Kent, A. G. *J. Chem. Soc., Perkin Trans. 2* **1987**, 1597.
(3) Moser, W. R.; Papile, C. J.; Brannon, D. A.; Duwell, R. A. *J. Mol. Catal.* **1987**, *41*, 271.
(4) Garland, M.; Bor, G. *Inorg. Chem.* **1989**, *28*, 410.
(5) Moasser, B.; Gladfelter, W. L. *Organometallics* **1995**, *14*, 3832.
(6) Schmid, R.; Herrmann, W. A.; Frenkling, G. *Organometallics* **1997**, *16*, 701.
(7) Matsubara, T.; Koga, N.; Ding, Y.; Musaev, D. G.; Morokuma, K. *Organometallics* **1997**, *16*, 1065.
(8) Diéguez, M.; Claver, C.; Masdeu-Bultó, A. M.; Ruiz, A.; van Leeuwen, P. W. N. M.; Schoemaker, G. C. *Organometallics* **1999**, *18*, 2107.
(9) Garland, M.; Pino, P. *Organometallics* **1991**, *10*, 1693.
(10) Feng, J.; Garland, M. *Organometallics* **1999**, *18*, 417.
(11) Castellanos-Páez, A.; Castillón, S.; Claver, C.; van Leeuwen, P. W. N. M.; de Lange, W. G. J. *Organometallics* **1998**, *17*, 2543.
(12) Iggo, J. A.; Shirley, D.; Tong, N. C. *New J. Chem.* **1998**, 1043.
(13) Evans, D.; Osborn, J. A.; Wilkinson, G. *J. Chem. Soc. A* **1968**, 3133.

10.1021/om000785h CCC: $20.00
Publication on Web 01/11/2001

Scheme 1. Hydroformylation Reaction Cycle

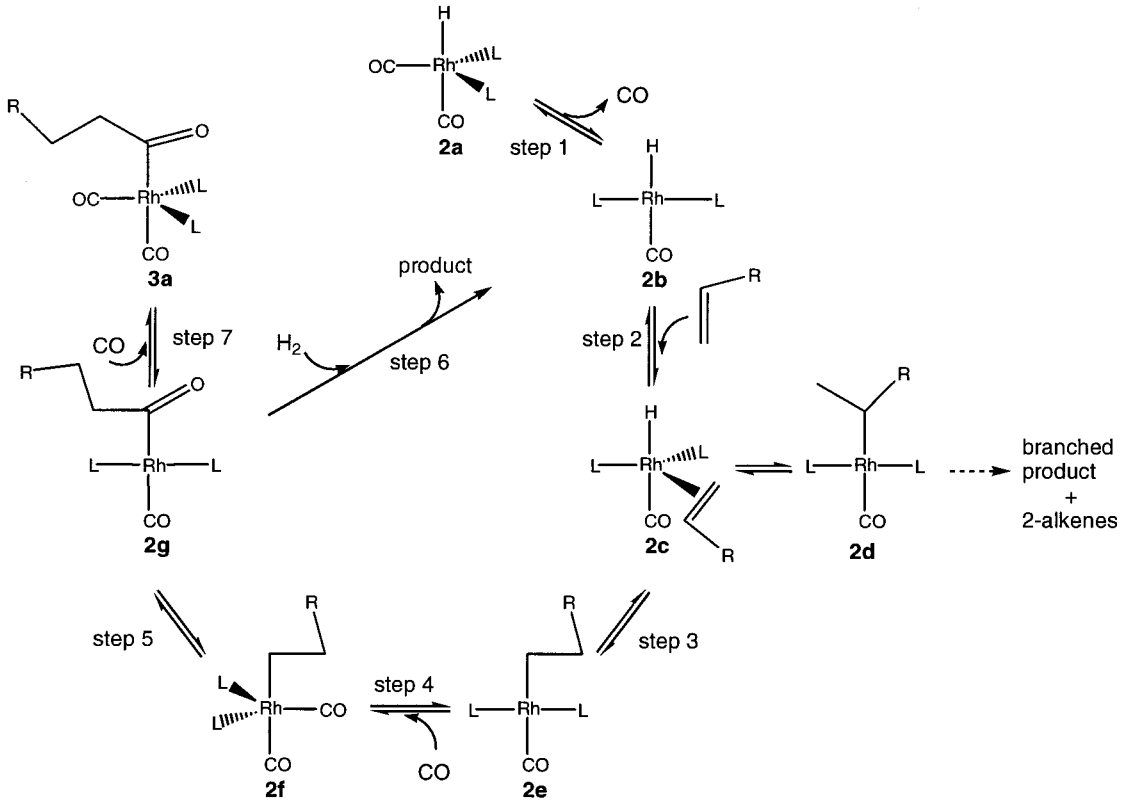

regeneration of the coordinatively unsaturated hydride complex **2b** and the production of either the linear or the branched aldehyde (step 6). Depending on the electronic and steric properties of the ligands used, different steps will control the reaction rate and different intermediates will be present in the reaction mixture as the catalyst resting state.

Many detailed studies on the reaction kinetics and the resting state of an *unmodified* rhodium carbonyl catalyst using various substrates have been performed.[9,10,14,15] These studies showed that the rate-determining step of the hydroformylation reaction for this electron-poor rhodium catalyst is hydrogenolysis. Garland and co-workers[9,16] identified a rhodium−acyl intermediate as the resting state of the catalyst using in situ IR spectroscopy. van Leeuwen et al.[17,18] investigated hydroformylation catalysts based on bulky monodentate phosphite ligands. Kinetic studies of the hydroformylation reaction catalyzed by this electron-poor rhodium catalyst revealed a zero order in alkene concentration and an approximate first-order rate dependency on the hydrogen concentration, indicating that the rate-determining step is the hydrogenolysis.[19] In situ IR studies confirmed this hypothesis by showing that the rhodium−acyl complex is present as the resting state of the catalyst during the hydroformylation reaction under these conditions.[20]

Despite their importance, very few kinetic studies have been performed on ligand modified hydroformylation rhodium catalysts. Cavalieri d'Oro and co-workers[21] investigated the reaction kinetics of a triphenylphosphine-modified catalyst, which were different from the kinetics of catalysts containing bulky phosphite ligands. This study showed that the rate equation for this system depends on the substrate and phosphine concentrations. The reaction showed a zero-order dependency on both CO and H_2 concentration. The selectivity for the linear aldehyde was found to depend dramatically on the ratio between CO and ligand concentrations. Wilkinson[22] and Brown[2] and co-workers examined the coordination chemistry of several rhodium−phosphine complexes that are potential intermediates in the hydroformylation reaction using IR and NMR spectroscopy. Under the conditions studied, $HRh(PPh_3)_2(CO)_2$ was present as the most abundant species during the hydroformylation reaction, as detected by in situ IR and NMR techniques.[23,24] Moser investigated the hydroformylation reaction intermediates formed from a range of para-substituted triphenylphosphine ligands.[3] From their data they concluded that when the electron density on rhodium is decreased, the rate-limiting step shifts from "just after the formation of $HRhL_2(CO)_2$ ($L = PPh_3$) to just after formation of $RhR(CO)_2L_2$ ($L = (p\text{-}ClPh)_3P$ or $L = (p\text{-}CF_3Ph)_3P$)".

Recently we reported on a new group of phosphorus diamides as ligands for the hydroformylation reaction

(14) Heil, B.; Markó, L.; Bor, G. *Chem. Ber.* **1971**, *104*, 3418.
(15) Vidal, J. L.; Walker, W. E. *Inorg. Chem.* **1981**, *20*, 249.
(16) Liu, G.; Volken, R.; Garland, M. *Organometallics* **1999**, *18*, 3429.
(17) van Leeuwen, P. W. N. M.; Roobeek, C. F. *J. Organomet. Chem.* **1983**, *258*, 343.
(18) Jongsma, T.; Challa, G.; van Leeuwen, P. W. N. M. *J. Organomet. Chem.* **1991**, *421*, 121.
(19) van Rooy, A.; Orij, E. D.; Kamer, P. C. J.; van Leeuwen, P. W. N. M. *Organometallics* **1995**, *14*, 34.
(20) van Rooy, A. *Thesis* **1995**, page 48.
(21) Cavalieri d'Oro, P.; Raimondi, L.; Pagani, G.; Montrasi, G.; Gregorio, G.; Andreetta, A. *Chim. Ind.* **1980**, *62*, 572.
(22) Yagupsky, G.; Brown, C. K.; Wilkinson, G. *J. Chem. Soc. A* **1970**, 1392.
(23) Morris, D. E.; Tinker, H. B. *CHEMTECH* **1972**, 554.
(24) Bianchini, C.; Man Lee, H.; Meli, A.; Vizza, F. *Organometallics* **2000**, *19*, 849.

Chart 1

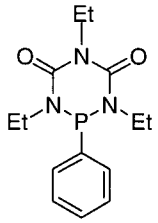

(**1**)

based on a 1,3,5-N,N′,N″-trisubstituted biuret structure.[25] These ligands combine the π-acidity of phosphites with the steric properties of phosphines. This unique combination of electronic and steric ligand properties leads to an increase of the hydroformylation activity in comparison to that of phosphine-based catalyst systems. Under hydroformylation reaction conditions, these bulky ligands formed exclusively the equatorial−equatorial rhodium−hydride complex; although the ligands are very bulky, the catalyst selectivity for the linear aldehyde remained moderate. This observation suggests that during the catalytic cycle an equatorial−apical complex might be formed. Here we present a mechanistic study using these phosphorus diamide ligands in order to understand the catalyst performance. The rate-limiting step in the hydroformylation reaction of 1-alkenes using ligand **1** (Chart 1) was investigated and the solution structure of the resting state of the catalyst was studied using (in situ) high-pressure spectroscopic techniques.

Results and Discussion

Kinetic Studies. The rate-controlling steps of the hydroformylation reaction of 1-octene using $HRh(\mathbf{1})_2(CO)_2$ (**2a**) were determined by a detailed kinetic study. In this study the concentration dependency of the reaction rate of all the reactants was investigated. The initial rate of aldehyde production was determined over the first 10% of conversion. Earlier research showed that ligand **1** can form mixtures of two different hydride complexes ($HRh(\mathbf{1})_2(CO)_2$ and $HRh(\mathbf{1})(CO)_3$) under hydroformylation conditions.[25] The performances of these two catalysts in the hydroformylation reaction are different. Therefore, the optimal rhodium and ligand concentrations were determined using high-pressure IR spectroscopy to ensure exclusive formation of $HRh(\mathbf{1})_2(CO)_2$.

One of the important side reactions obtained under hydroformylation reaction conditions is the dimerization reaction depicted in Scheme 2. High rhodium and low H_2 concentrations and low temperatures promote the formation of these dimeric rhodium complexes.[11,26,27] To investigate the effect of the rhodium concentration on the reaction rate, we varied this concentration between 0.5 and 4 mM (see Figure 1). The rate of aldehyde production is linearly proportional to the rhodium concentration. This first-order dependency indicates that dimerization of the rhodium complexes is not involved under the applied hydroformylation conditions using ligand **1**.

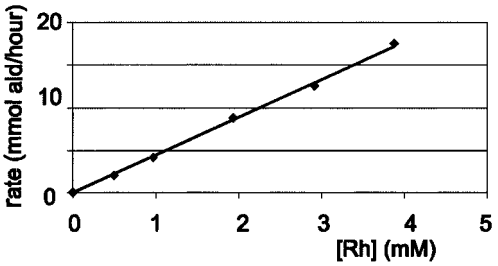

Figure 1. Variation of the rhodium concentration. Conditions: T = 41 °C, $p_{CO} = p_{H_2}$ = 10 bar, [L] = 19 mM, [1-octene] = 0.59 M. Values of the rate are least-squares fits ($r^2 \geq 0.998$) of lines from plots of millimoles of aldehyde vs time over 0−10% conversion.

Scheme 2. Equilibrium between Monomeric and Dimeric Rhodium Complexes

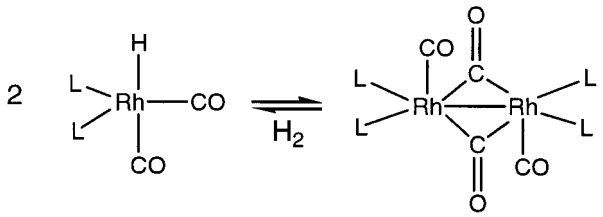

Table 1. Substrate Concentration Dependency on the Hydroformylation Reaction Rate[a]

[1-octene] (M)	conversn (%)	k_{ald}[b]	l/b (%)	2-octene (%)
0.44	22	152	1.7	2
0.59	13	165	1.7	2
0.59	20	162	1.7	1
0.88	25	183	1.9	2
1.18	23	201	1.9	1

[a] Conditions: T = 41 °C, $p_{CO} = p_{H_2}$ = 10 bar, [Rh] = 1.9 mM, [ligand] = 19 mM. Samples were taken between 0 and 10% conversion. [b] In units of (mol of aldehyde) (mol of Rh)$^{-1}$ h^{-1} averaged over time.

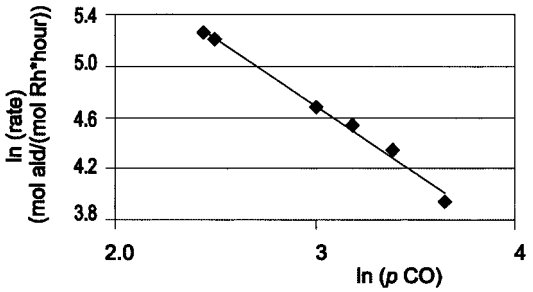

Figure 2. Variation of the partial CO pressure. Conditions: T = 41 °C, [Rh] = 2 mM, Rh/L = 1/10, p_{H_2} = 10 bar, [1-octene] = 0.59 M. Values of the rate are least-squares fits ($r^2 \geq 0.998$) of lines from plots of millimoles of aldehyde vs time over 0−10% conversion.

The 1-octene concentration was varied between 0.4 and 1.2 M. The results depicted in Table 1 show a rate dependency of 0.3. The partial CO pressure was varied between 10 and 35 bar. The natural logarithm plot of the reaction rate against the partial CO pressure shows a negative first-order dependency on the partial CO pressure (see Figure 2). The partial hydrogen pressure was varied between 10 and 40 bar (Table 2). The natural

(25) van der Slot, S. C.; Kamer, P. C. J.; van Leeuwen, P. W. N. M.; Fraanje, J.; Goubitz, K.; Lutz, M.; Spek, A. L. *Organometallics* **2000**, *19*, 2504.
(26) Evans, D.; Yagupsky, G.; Wilkinson, G. *J. Chem. Soc. A* **1968**, 2660.
(27) James, B. R.; Mahajan, D.; Rettig, S. J.; Williams, G. M. *Organometallics* **1983**, *2*, 1452.

Table 2. CO and H_2 Partial Pressure Dependency on the Hydroformylation Reaction Rate[a]

p_{H_2}(bar)	p_{CO}(bar)	conversn (%)	k_{ald}[b]	l/b (%)	2-octene (%)
10.5	11.5	25	191	1.7	2
10.6	12.1	23	183	1.8	3
10.6	20.2	20	108	1.7	3
10.5	24.3	23	93	1.8	2
10.0	29.5	29	77	1.7	2
10.6	38.5	18	52	1.7	2
11.8	10.6	26	193	1.8	3
18.1	10.5	26	263	1.8	3
29.9	10.3	24	407	1.8	1
34.7	10.5	24	456	1.8	2

[a] Conditions: T = 41 °C, [Rh] = 1.9 mM, [ligand] = 19 mM, [1-octene] = 0.59 M. Samples were taken between 0 and 10% conversion. [b] In units of (mol of aldehyde) (mol of Rh)$^{-1}$ h^{-1} averaged over time.

Table 3. Ligand Concentration Dependency on the Hydroformylation Reaction Rate[a]

[L] (mM)	conversn (%)	k_{ald}[b]	l/b (%)	2-octene (%)
19	25	226	1.9	2
29	28	206	1.9	2
37	26	191	1.9	2
49	25	183	1.9	2
67	22	165	2.0	2

[a] Conditions: T = 41 °C, $p_{CO} = p_{H_2}$ = 10 bar, [Rh] = 1.9 mM, [1-octene] = 0.59 M. Samples were taken between 0 and 10% conversion. [b] In units of (mol of aldehyde) (mol of Rh)$^{-1}$ h^{-1} averaged over time.

logarithm plot of the reaction rate against the partial hydrogen pressure shows a large positive (0.8) dependency on the hydrogen pressure. We studied the effect of the ligand concentration on the reaction rate by varying this concentration between 19 and 67 mM. The results show a rate dependency of −0.3 (Table 3).

The positive reaction order found for the alkene concentration and the negative reaction order found for the CO pressure and ligand concentration are similar to the results found for the triphenyl phosphine based catalyst.[21] The rate equation for this type of kinetics, as proposed by van Leeuwen et al.[28] as type I kinetics, is

$$\text{rate(type I)} = \frac{A[\text{Rh}][\text{alkene}]}{B[\text{CO}] + C[\text{alkene}] + [\text{L}]} \qquad \text{(I)}$$

Rate-influencing reactions are CO or ligand dissociation, alkene coordination, and hydride migration. The resting state of the catalyst fitting this kinetics is the rhodium−hydride complex **2a**. Type I kinetics is observed for most ligand-modified rhodium catalysts. The large positive reaction order found for the hydrogen pressure suggests that the hydrogenolysis step is also important in determining the overall reaction rate. The rate equation fitting these results which were proposed as Type II kinetics is[28]

$$\text{rate(type II)} = \frac{D[\text{Rh}][\text{H}_2]}{E[\text{CO}] + F[\text{H}_2] + [\text{L}]} \qquad \text{(II)}$$

Coordinatively saturated rhodium−acyl complexes such as **3a** will be present in the reaction mixture as resting states of the catalyst.

The kinetic data obtained for **2a** show that the rate-determining step of the hydroformylation reaction using this catalyst cannot be reduced to one single step of the

Scheme 3

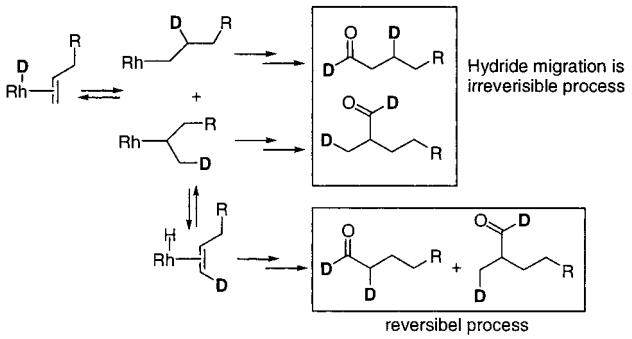

hydroformylation mechanism. Several reaction steps in the proposed mechanism are involved controlling the reaction rate. The alkene coordination/hydride migration and the hydrogenolysis have very similar rates leading to a combination of the type I and type II kinetics, as given in eq III, of the overall reaction rate

$$\text{rate(overall)} = \frac{G[\text{Rh}][\text{H}_2][\text{alkene}]}{H[\text{CO}] + K[\text{alkene}] + [\text{H}_2]} \qquad \text{(III)}$$

of the approximate form. The overall reaction rate is strongly dependent on the reaction conditions used. At high hydrogen pressure, the catalyst will show type I kinetics: i.e. the alkene coordination/hydride migration determines the overall rate of reaction. When the alkene concentration is increased, the catalyst will show type II kinetics: i.e., the hydrogenolysis determines the overall reaction rate. Therefore, noninteger reaction orders given above are valid only within the window of the concentration and pressure ranges studied. As a result of these kinetics, both rhodium−hydride and rhodium−acyl complexes (**2a**, **3a**) are expected to be present under the conditions studied.

Deuterioformylation Reaction. To determine the reversibility of the alkene coordination and hydride migration, we performed a deuterioformylation experiment.[29,30] If rhodium−alkyl formation by hydride migration to the coordinated alkene is irreversible, then the aldehydes will contain deuterium labels on the aldehyde carbon atom and the β-carbon atom. Reversible rhodium−alkyl formation will result in α-deuteration (see Scheme 3). If alkene coordination and hydride migration are both reversible and fast, then deuterium will be incorporated into the alkene and the number of deuterium labels present in the aldehyde molecule will differ in part from 2. The deuterioformylation was performed under the same conditions as the hydroformylation experiments (T = 41 °C, [Rh] = 1.9 mM, Rh/L = 1/10, [1-hexene] = 0.81 M, $p_{CO} = p_{D_2}$ = 10 bar). 1-Hexene was used for the deuterioformylation instead of 1-octene to facilitate comparison with literature data of the ^{1}H and ^{2}H NMR spectra.[29] The rates and selectivity for 1-hexene are comparable with those of 1-octene. The production of aldehydes was monitored by gas

(28) van Leeuwen, P. W. N. M.; Casey, C. P.; Whiteker, G. T. In *Rhodium Catalysed Hydroformylation*; van Leeuwen, P. W. N. M., Claver, C., Ed.; Kluwer Academic: Dordrecht, The Netherlands, 2000; Chapter 4.

(29) Casey, P. C.; Petrovich, L. M. *J. Am. Chem. Soc.* **1995**, *117*, 6007.

(30) Lazzaroni, R.; Uccello-Barretta, G.; Benetti, M. *Organometallics* **1989**, *8*, 2323.

chromatography. The number of deuteriums incorporated into 1-hexene, heptanal, and 2-methylhexanal was monitored by gas chromatography/mass spectroscopy. The activity and selectivity for the deuterioformylation of 1-hexene were similar to those of the hydroformylation of 1-hexene. Gas chromatography/mass spectroscopy showed hardly any deuterium enrichment at low conversions of 1-hexene. At higher conversion (≥95%), a slight deuterium enrichment of *n*-hexene (∼3%) was observed, which is due to the increasing concentration of the less reactive 2-alkenes at high conversions. Two deuterium labels were incorporated in the aldehyde molecules. This suggests that β-hydride elimination and alkene dissociation occur only in very few occasions. The linear and branched aldehydes were separated from the reaction mixture by distillation and column chromatography after complete conversion of 1-hexene. The deuterium distribution was determined using ^{1}H and ^{2}H NMR spectroscopy. We were not able to detect aldehydes containing the deuterium on the α-carbon atom using ^{1}H NMR spectroscopy. The ^{2}H NMR spectrum of the mixture of the linear and branched aldehydes shows deuterium labels exclusively at the aldehyde carbon and β-carbon atoms. Similar to the results of Casey and Petrovich[29] obtained for the bidentate phosphine ligands, a deuterium label at the α-carbon was not observed within the detection limits of ^{2}H NMR spectroscopy. Therefore, we conclude that for this ligand, under the conditions studied, hydride migration is virtually an irreversible process. Probably, the alkene dissociation is much faster than the hydride migration. For a small percentage of molecules that do undergo β-hydride elimination, the alkene dissociates before hydride migration occurs again. Both linear and branched rhodium−alkyl complexes are formed irreversibly, and therefore the regioselectivity of the reaction is determined in the hydride migration step.

In Situ IR Studies. In the previous section, we showed that several elementary reaction steps of the hydroformylation reaction influence the overall reaction rate. On the basis of these results rhodium−hydride and rhodium−acyl complexes were proposed to be present as potential "resting" states during the hydroformylation reaction. The complexes present were investigated using in situ spectroscopic techniques. The results obtained in the in situ HP IR experiments are presented in Table 4. In a typical experiment the hydride complex **2a** was formed in situ, and after addition of 1-octene the hydroformylation reaction was monitored using a rapid scan IR technique (7 scans/s). The difference spectra obtained (Figure 3) show negative absorption bands for the carbonyl frequencies of complexes that are converted (in part) to other complexes after addition of the substrate. Positive absorption bands are obtained for carbonyl frequencies of complexes that are formed during the hydroformylation reaction. The rhodium hydride complex **2a** (ν_{CO} = 2070, 2018 cm^{-1}; Table 5) is the only rhodium complex present in all experiments, both before addition and after complete conversion of 1-octene. The difference IR spectra show absorption bands in the terminal carbonyl region only. No absorptions of bridging carbonyls are observed, which confirms that inactive rhodium dimers or clusters are not present during the reaction, as already concluded from the first-order rate dependency on the rhodium concentration observed in the kinetic experiments.

Table 4. Absorptions Obtained from in Situ IR Experiments

			ν_{CO} (cm^{-1})[a]	
p_{CO} (bar)	p_{H_2} (bar)	[1-octene] (M)	disappearing[b]	appearing[b]
7	7	0.2	2070 (**2a**) 2018 (**2a**)	2085 (w) 2077 (sh) 2028 (w) 2010 (sh) 2001 (m) 1991 (m) 1967 (w)
7	32	0.2	−	−
7	7	0.6	2070 (**2a**) 2018 (**2a**)	2085 (w) 2077 (sh) 2028 (w) 2010 (sh) 2001 (m) 1991 (m) 1967 (w)

[a] All experiments were performed in cyclohexane at 40 °C. [b] Appearing absorption bands are obtained for carbonyl frequencies of complexes that are formed during the hydroformylation reaction; disappearing absorption bands are obtained for carbonyl frequencies of complexes that are converted to other complexes.

The kinetic experiments indicate the presence of both coordinatively saturated rhodium−hydride and rhodium−acyl complexes during the hydroformylation. The spectroscopic data of several rhodium−hydride complexes obtained with ligand **1** are depicted in Table 5. Rhodium−hydride complexes containing two phosphorus ligands can have either equatorial−equatorial (ee) or equatorial−apical (ea) coordinated phosphorus ligands.[31] The formation of the ea isomer is not likely since complexes with ea coordinated phosphorus ligands were never observed under hydroformylation conditions using ligand **1**.[25] Immediately after addition of 1-octene, the strong absorption band of nonanal (1734 cm^{-1}) appeared in the IR spectrum, proving that the hydroformylation reaction has started. The amount of **2a** dropped considerably upon addition of 1-octene. However, comparing the intensity of the carbonyl frequencies of **2a** before and after addition of 1-octene showed that **2a** was still present in low concentration during the hydroformylation reaction. Seven new absorptions appeared in the terminal carbonyl region, indicating that complex **2a** was converted (in part) to several new carbonyl-containing rhodium complexes. Only one rhodium−hydride complex was observed during the hydroformylation reaction, the rhodium−hydride complex containing two phosphorus diamide ligands (Table 5).

The kinetic experiments showed that the hydrogenolysis (step 6, Scheme 1) is a relatively slow step in the hydroformylation reaction and rhodium−acyl complexes are expected to be present during the hydroformylation reaction. Several possible structures of rhodium−acyl complexes are depicted in Figure 4. Since the catalyst does not show high selectivity for the linear aldehyde, it can be concluded that both the linear and branched rhodium−acyl complexes are formed (**3a**,**b**). Coordination of one of the phosphorus atoms at an apical position leading to ea coordinated complexes is

(31) van der Veen, L. A.; Boele, M. D. K.; Bregman, F. R.; Kamer, P. C. J.; van Leeuwen, P. W. N. M.; Goubitz, K.; Fraanje, J.; Schenk, H.; Bo, C. *J. Am. Chem. Soc.* **1998**, *120*, 11616.

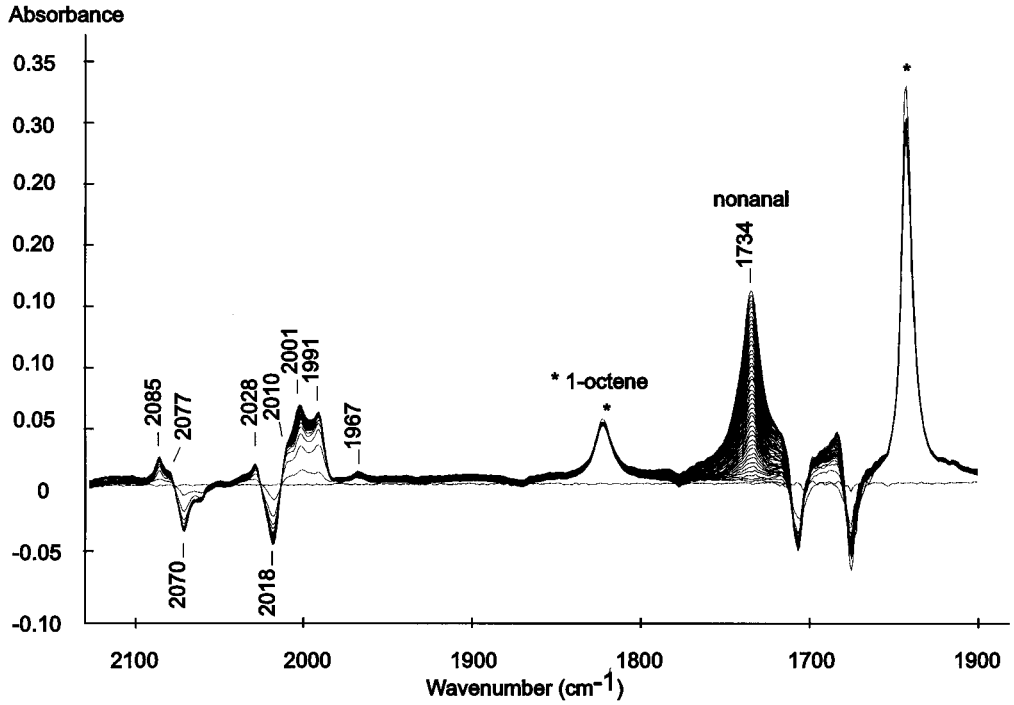

Figure 3. Difference spectrum of the in situ IR experiment.

Table 5. NMR and IR Data HRh(1)$_x$(CO)$_{4-x}$ (x = 1−3) Complexes

compd	$\delta(^1H)^a$ (ppm)	$\delta(^{31}P)^a$ (ppm)	$\delta(^{13}CO)^a$ (ppm)	coupling constants (Hz)	ν_{CO} (cm^{-1})^b
HRh(**1**)(CO)$_3$	−10.3	104	nd^c	$J_{RhH} \leq 3$, $J_{RhP} = 177$, $J_{PH} = 15$	2095, 2045, 2008
HRh(**1**)$_2$(CO)$_2$ (**2a**)	−10.6 (broad)	110	194^d	$J_{RhH} \leq 3$, $J_{RhP} = 181$, $J_{CP} = 22$, $J_{RhC} = 58$, $J_{CH} = 16$, $J_{PH} \leq 3$	2070, 2018
HRh(**1**)$_3$CO	−11.1	117	200	$J_{RhH} \leq 3$, $J_{RhP} = 169$, $J_{PH} = 13$, $J_{CP} = 13$, $J_{RhC} = 52$, $J_{CH} = 36$	2019

^{a} All NMR experiments were performed in toluene-d_8. ^{b} Measured in cyclohexane. ^{c} Not determined. ^{d} The equatorial and apical carbonyl ligands are in fast exchange under the conditions studied.

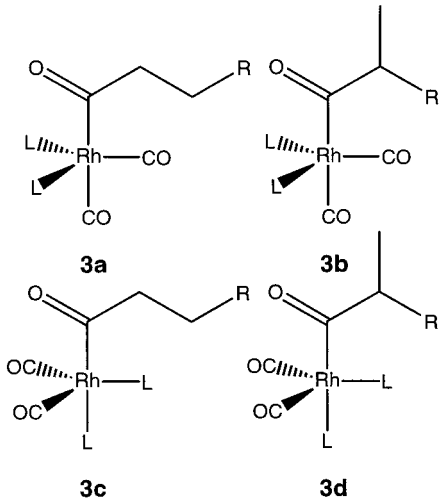

Figure 4. Possible structures of rhodium acyl complexes.

also possible. The ea coordination mode has not been observed for the hydride complex (**2a**), but coordination of the larger acyl moiety at one of the apical positions can lead to distortion of the trigonal-bipyramidal structure or coordination of a phosphorus ligand trans to the acyl ligand. The new carbonyl bands obtained in the IR spectrum probably belong to several of the rhodium−acyl complexes, as depicted in Figure 4. The strong amide bands of the ligand in this region obscure the expected rhodium−acyl absorption band[10,20] around 1600−1700 cm^{-1}. Therefore, the absorption of rhodium−acyl species could not be observed in the IR spectra.

Rhodium hydride complex **2a** was the only rhodium complex observed during the hydroformylation reaction when the partial hydrogen pressure was increased to 32 bar (Table 4). Higher hydrogen pressures facilitate the hydrogenolysis step, and the simplified type I kinetic equation becomes valid (vide supra). The absence of terminal carbonyl bands in the difference IR spectra observed under high partial hydrogen pressure indicates that under these conditions only the rhodium−hydride complex **2a** is present. The amount of **2a** decreased and the intensity of the additional carbonyl bands increased with increasing alkene concentration. This indicates that at higher alkene concentration the contribution of the hydrogenolysis step as the rate-controlling step increases, finally resulting in type II kinetics. The shift of rate control, depending on the conditions used, shows that the rate expression of this catalyst system is strongly dependent on the conditions used.

Stoichiometric Reactions. The hydroformylation reaction was investigated in a stepwise manner by the subsequent reactions of **2a** with alkene, CO, and H_2 in an attempt to characterize the complexes formed during the hydroformylation reaction. In the absence of H_2, complex **2a**, alkene, and CO can undergo all hydroformylation reaction steps except the hydrogenolysis step and rhodium−acyl complexes may be formed. The IR data obtained after the subsequent reaction steps are

Table 6. IR Frequencies Obtained in the Stoichiometric Reaction of 2a, 1-Octene, CO, and H_2

conditions[a]	ν_{CO} (cm^{-1})
2a under 5 bar of CO	2080, 2017
2a + 25 equiv of 1-octene under 5 bar of CO	2085 (w), 2077 (sh), 2028 (w), 2010 (sh), 2001 (m), 1991 (m), 1967 (w)
2a + 25 equiv of 1-octene under 10 bar of CO/H_2 (1/1)	2080, 2017

[a] All reactions were performed in cyclohexane at room temperature.

presented in Table 6. The carbonyl frequencies obtained after the reaction of **2a**, 1-octene, and CO were identical with those obtained in the in situ IR experiments obtained during the hydroformylation reaction, except for the absence of the carbonyl frequency due to the aldehyde. Subsequent addition of hydrogen showed aldehyde formation, and after all the 1-octene was converted, **2a** was the only complex present again. Therefore, we conclude that the complexes formed in the stoichiometric reaction of **2a**, alkene, and CO are equal to the most abundant complexes present during the hydroformylation reaction at low H_2 pressure. This indicates that in this instance the stoichiometric reaction is an elegant and reliable method to study the intermediates of the hydroformylation reaction in a stationary system.

NMR Study of the Complexes Obtained in the Stoichiometric Reaction. High-pressure (HP) NMR spectroscopy is a powerful technique to determine the precise structure of complexes present during the hydroformylation reaction. Higher sample concentrations and longer collection times are needed for NMR studies. The stoichiometric hydroformylation of 1-hexene using NMR spectroscopy was investigated using the same procedure as that for the IR experiments. The experiments were performed in a high-pressure NMR flow cell as described by Iggo and co-workers.[12] The advantages of an HP flow cell instead of an HP NMR tube[32] are the continuous supply of reactants and optimal mixing of the reactants (minimization of diffusion problems). Homogeneously catalyzed reactions can be monitored using this flow cell, and stable intermediates can be characterized using different NMR techniques.

Rhodium complex **2a** was prepared in situ in the NMR cell from the rhodium precursor ($Rh(acac)(CO)_2$) and 5 equiv of ligand **1** by heating at 80 °C for 1 h under 20 bar of CO/H_2 (1/1) (spectrum a, Figure 5). Complex **2a** is the only rhodium complex obtained according to the ^{31}P NMR spectrum. The hydrogen gas was removed by bubbling CO through the solution for 30 min at 253 K. Approximately 25 equiv of 1-hexene was injected into the NMR cell at 253 K, and the solution was warmed slowly to room temperature. When the temperature was raised, the ^{31}P NMR spectrum started to broaden and both the ^1H NMR and ^{31}P NMR spectra showed that the resonance due to the hydride complex decreased in intensity. To trap all complexes present, the solution was cooled immediately to 253 K. This results in NMR spectrum b as presented in Figure 5. The spectrum at this temperature showed an additional (broad) doublet (δ 109.5 ppm, $J_{RhP} = 205$ Hz) upfield from the doublet

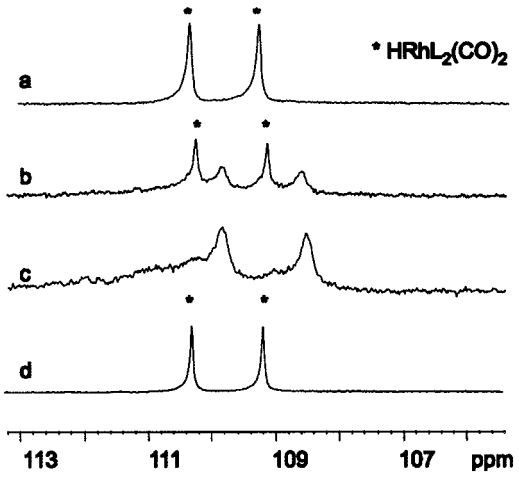

Figure 5. Overview of the $^{31}P\{^1H\}$ NMR spectra of the stepwise reaction of **2a**, 1-hexene, and CO with H_2: (a) $^{31}P\{^1H\}$ NMR spectrum of **2a** under 5 bar of CO; (b) $^{31}P\{^1H\}$ NMR spectrum of **2a** in the presence of 5 bar of CO and 25 equiv of 1-hexene; (c) $^{31}P\{^1H\}$ NMR spectrum after complete conversion of **2a**; (d) $^{31}P\{^1H\}$ NMR spectrum after addition of 5 bar of CO/H_2 (1/1). All spectra were recorded at 253 K.

of **2a** (spectrum b, Figure 5). Complex **2a** was converted almost completely to the new compounds by warming the solution to room temperature again. The additionally formed doublet is only visible at 253 K (spectrum c, Figure 5). A broad resonance appeared downfield from the doublet, indicating that probably more than one complex was present (a major and a minor complex). The ^{31}P NMR spectrum at room temperature showed a very broad peak at the position of the free ligand (64 ppm), indicating that the coordinated phosphorus ligands are in exchange with the free phosphorus ligand. The hydride resonance in the ^1H NMR spectrum has disappeared, and no aldehyde resonance was observed. We were not able to obtain a sharp ^{31}P resonance of the doublet formed under these conditions because of the temperature limits of the NMR flow cell. When the gas flow was changed from 5 bar of CO to 5 bar of CO/H_2 (1/1), the broad doublet in the phosphorus NMR spectrum disappeared and the characteristic doublet due to the hydride complex **2a** was observed (spectrum d, Figure 5). The ^1H NMR spectrum showed the reappearance of the hydride resonance at −10.6 ppm together with an aldehyde resonance at 9.3 ppm. Repeating this sequence using this NMR sample gave the same results, indicating the retention of activity for the rhodium−catalyzed reaction. These results confirm that the complex formed in the absence of H_2 is an intermediate of the hydroformylation reaction.

The new complexes could also be prepared in an NMR tube, and they are stable for several days under 3 bar of CO at 193 K. The ^{31}P NMR spectrum showed again a very broad resonance at the position of the free ligand at room temperature. When the sample was cooled to 253 K, the ^{31}P NMR spectrum showed the appearance of the broad doublet at 109.5 ppm ($J_{RhP} = 205$ Hz) together with a broad resonance downfield from this doublet. The spectrum broadened when the temperature was decreased. The ^{31}P NMR spectrum obtained at 193 K will be discussed in more detail later.

(32) Elsevier, C. J. *J. Mol. Catal.* **1994**, *92*, 285.

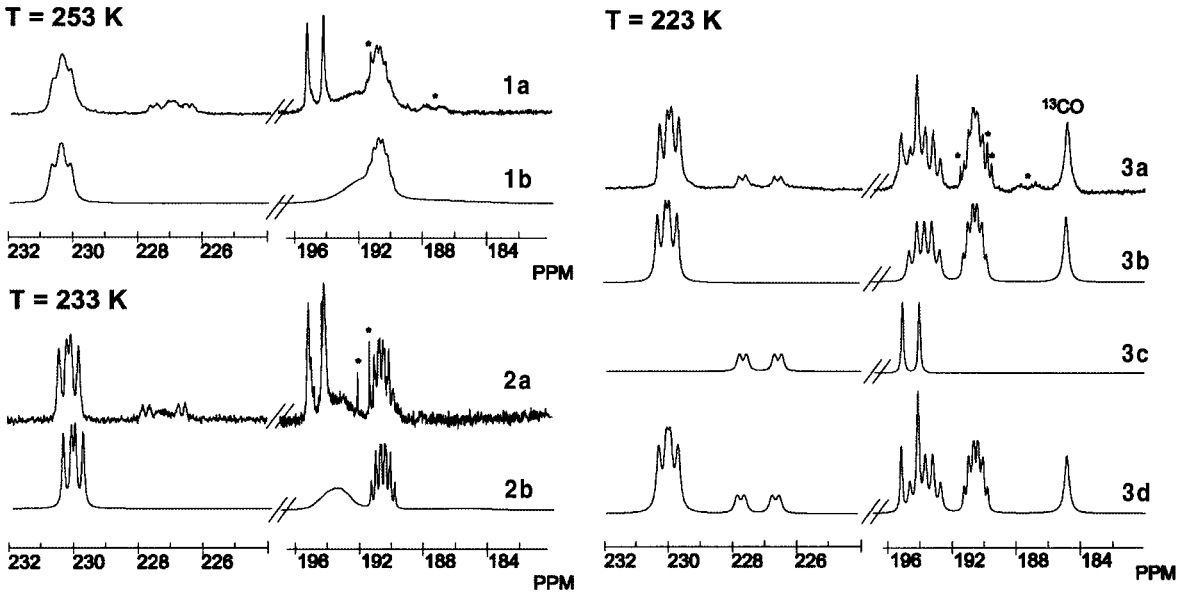

Figure 6. Variable-temperature $^{13}C\{^1H\}$ NMR spectra obtained after the reaction of **2a**, 1-hexene, and CO: (1a) $^{13}C\{^1H\}$ NMR spectrum obtained at 253 K; (1b) simulation of the $^{13}C\{^1H\}$ NMR spectrum of 1a; (**2a**) $^{13}C\{^1H\}$ NMR spectrum obtained at 233 K; (2b) simulation of the $^{13}C\{^1H\}$ NMR spectrum 2a; (3a) $^{13}C\{^1H\}$ NMR spectrum obtained at 223 K; (3b) simulation of $^{13}C\{^1H\}$ NMR spectrum 3a at 223 K; (3c) simulation of $^{13}C\{^1H\}$ NMR spectrum 3c at 223 K; (3d) simulation of the $^{13}C\{^1H\}$ NMR spectrum obtained at 223 K of **3a**:**3d** = 1:0.4. The asterisk denotes an impurity.

The in situ IR experiments revealed that rhodium−acyl complexes may be formed in the reaction of **2a**, 1-hexene, and CO. Rhodium−acyl carbon atoms have characteristic chemical shifts in the ^{13}C NMR spectrum around 235 ppm. Therefore, the reaction was performed with ^{13}CO to enable the identification of the rhodium−acyl resonance in ^{13}C NMR. Figure 6 shows an overview of the $^{13}C\{^1H\}$ NMR spectra obtained in a variable-temperature experiment. All the resonances in the ^{13}C NMR spectrum were very broad at room temperature. The resonances sharpened when the temperature was decreased. This indicates that several intra- and intermolecular exchange processes are involved (vide infra). The ^{13}C NMR spectrum at 223 K (spectrum 3a, Figure 6) showed two rhodium−acyl resonances (δ 230.0 ppm and δ 227.2 ppm) and three different rhodium−carbonyl resonances (δ 194.7 ppm, δ 193.7 ppm and δ 190.6 ppm), indicating that we are dealing with two different rhodium−acyl complexes. The structures of these two rhodium−acyl complexes will be discussed in the following sections.

Characterization of Rhodium−Acyl Complexes 3a,b. The $^{13}C\{^1H\}$ NMR spectrum at 253 K (spectrum 3a, Figure 6) showed two rhodium−acyl resonances and three different rhodium−carbonyl resonances. The ^{13}C COSY90 spectrum showed strong cross-peaks of the carbonyl ligand at δ 193.7 and 190.6 ppm and weak cross-peaks for the carbonyl ligand at δ 190.6 ppm and the rhodium−acyl resonance at δ 230.0 ppm. Therefore, we conclude that these three carbonyl resonances belong to the same rhodium−acyl complex. We were not able to obtain information about the rhodium−acyl resonance at δ 227.2 ppm and the terminal CO resonance at δ 194.7 ppm using two-dimensional NMR techniques, because of the low concentration of this complex. Selective decoupling of the phosphorus resonance at δ 109 ppm at 233 K led to simplification of the carbon NMR spectrum to doublets of doublets for the acyl resonance at 230.0 ppm and the carbonyl resonance at 190.6 ppm. From this spectrum the rhodium−carbon coupling constants were calculated to be 18 Hz for the acyl carbon and 42 Hz for the carbonyl ligand. This spectrum also shows the two-bond carbonyl−acyl coupling constant of 28 Hz. The large $^2J_{CC}$ coupling constant of 28 Hz is indicative of a trans orientation of the carbonyl ligand and the acyl ligand.

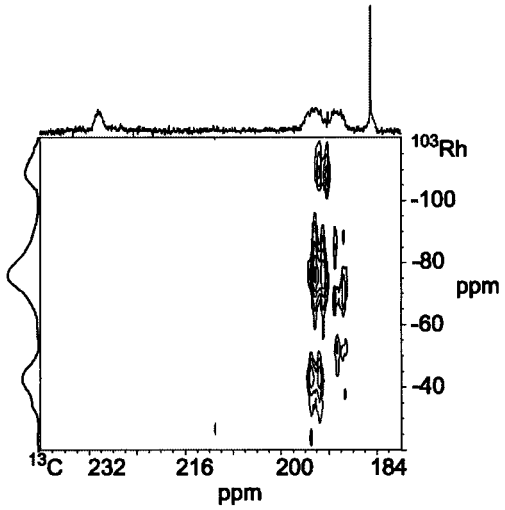

Figure 7. $^{103}Rh-^{13}C$ HMQC spectrum recorded at 183 K. The delay time $\tau = 1/[2J_{RhC}]$ calculated from $J_{RhC} = 70$ Hz was used.

Several $^{103}Rh-^{13}C$ HMQC spectra were recorded using different delay times ($\tau = 1/[2J_{RhC}]$). Figure 7 shows the $^{103}Rh-^{13}C$ HMQC spectrum obtained using a delay time τ calculated from $J_{RhC} = 70$ Hz. The carbonyl resonance at 193.7 ppm showed cross-peaks with a rhodium resonance at approximately −70 ppm. The multiplicity of the rhodium resonance (triplet) shows that two phosphorus atoms with approximately equal J_{RhP} coupling constants are coordinated to the

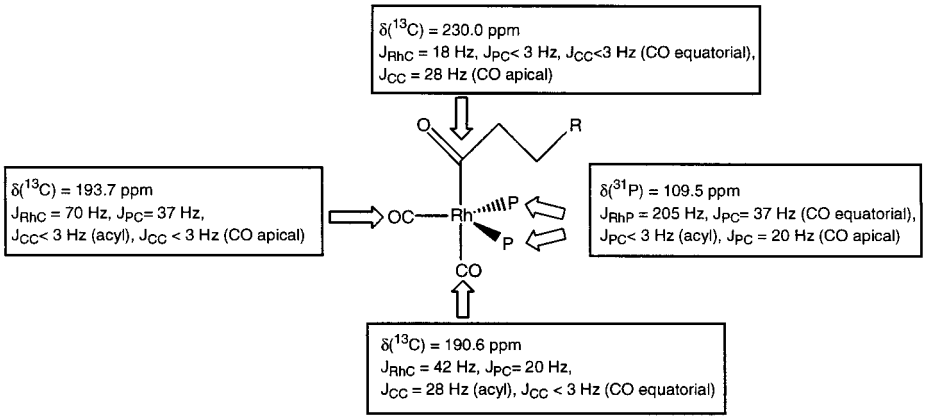

Figure 8. NMR data for the major rhodium−acyl complex formed in the reaction of **2a**, 1-hexene, and CO.

rhodium nucleus. Cross-peaks were obtained for the carbon resonances at 190.6 and 230.0 ppm and the triplet at ∼−70 ppm in the rhodium dimension in the ^{103}Rh−^{13}C HMQC spectrum when a delay time τ calculated from $J_{RhC} = 40$ Hz was used. A rhodium resonance at the same chemical shift was observed in the ^{103}Rh−^{31}P HMQC spectrum. From the results of the various NMR experiments we conclude that the major complex obtained at 223 K after reaction of **2a**, 1-hexene, and CO is a rhodium−acyl complex having two equatorially coordinated phosphorus ligands and two magnetically inequivalent carbonyl ligands. The precise NMR data obtained after simulation are presented in Figure 8; the simulated ^{13}C{^{1}H} NMR spectrum corresponding to these data is presented in Figure 6 (spectrum 3b). The two phosphorus atoms are coordinated in the equatorial plane of the trigonal-bipyramidal structure. The carbon resonance at 193.7 ppm shows a large coupling constant to the phosphorus nuclei (37 Hz), as also reported for equatorial carbonyl ligands in rhodium−hydride complexes (HRhL⁀L(CO)$_2$, L⁀L = bidentate phosphite ligand).[33] The large coupling constant of the equatorial carbonyl to the rhodium nucleus ($^1J_{CRh} = 70$ Hz) has also been reported by Brown and Kent.[2] The cis coupling of the carbonyl with the acyl carbon resonance is unresolved. The magnitude of the carbon−phosphorus coupling constant for the apical carbonyl (20 Hz) is larger than normally observed for $^2J_{CP}$ in a pure cis orientation. This relatively large $^2J_{CP}$ might be explained by distortion of the trigonal-bipyramidal structure. This is not unlikely, since distortion of the trigonal-bipyramidal structure is also observed for hydride complexes containing bulky monodentate and bidentate phosphite and phosphorus diamide ligands.[25,33]

Characterization of Rhodium−Acyl Complexes 3c,d. The second (minor) acyl resonance in the carbon NMR spectrum at δ 227.2 ppm shows a double triplet at 253 K (Figure 6, spectrum 1a). Selective decoupling of the phosphorus resonance at 109 ppm led to simplification of the acyl resonance to a doublet ($J_{RhC} = 17$ Hz). This indicates that the acyl resonance belongs to a complex that contains two (time-averaged) equivalent phosphorus atoms. The J_{CC} coupling constant of the acyl resonance and the carbonyl ligands is small, indicative of a cis relation. When the temperature was decreased, the phosphorus atoms lost their time-averaged equivalence. At 223 K, the slow-exchange region was reached and a doublet of doublets appeared at δ 227.2 ppm ($J_{RhC} = 17$ Hz, $J_{CP} = 83$ Hz, $J_{CP'} \leq 3$ Hz). Simulation using these data results in spectrum 3c (Figure 6). This acyl resonance belongs to a complex that contains one equatorial and one apical phosphorus atom (**3c**,**d**, Figure 4). A similar complex for triphenylphosphine has been reported by Brown and Kent.[2] The two carbonyl ligands in the equatorial plane show a sharp doublet in the terminal carbonyl region (δ 194.7 ppm, $J_{RhC} = 79$ Hz). The terminal carbonyls exhibit equal coupling constants to both phosphorus nuclei due to intramolecular exchange of the phosphorus atoms. When the temperature is decreased, the terminal carbonyl resonance broadened, and at 193 K a multiplet was observed. The J_{CP} coupling constants could not be resolved because of the overlap of this resonance and the terminal carbonyl resonance of the other acyl complex.

Summarizing, we conclude that in the reaction of **2a**, 1-hexene, and CO, two rhodium−acyl complexes are formed. Spectrum 3d (Figure 6) shows the complete simulation of the ^{13}C{^{1}H} NMR spectrum obtained at 223 K. The ^{13}C{^{1}H} NMR spectrum contains both rhodium−acyl complexes **3a**,**b** and **3c**,**d** in a ratio of 1 to 0.4. Both rhodium−acyl complexes have a trigonal-bipyramidal structure with the acyl moiety coordinated at an apical position. Both complexes contain two phosphorus ligands and two carbonyl ligands. The major complex formed contains two phosphorus ligands coordinated in the equatorial plane of the trigonal bipyramid; the minor complex has one phosphorus atom coordinated at an equatorial position and one at an apical position of the trigonal bipyramid. In Figure 4, we proposed four different structures for the acyl complexes present (**3a**−**d**). On the basis of the NMR data obtained, we are not able to distinguish between the linear- and branched-acyl structures. However, since the branched-acyl ligand introduces more steric hindrance close to the rhodium center than the linear-acyl ligand, it is tempting to suggest that the major rhodium−acyl complex contains a linear acyl ligand (complex **3a**), whereas the minor rhodium−acyl complex contains a more bulky branched acyl ligand (complex **3d**). The linear-to-branched ratio found in the catalytic reaction cannot be explained by the ratio of **3a** to **3d** found in the NMR experiments, because these two

(33) van Rooy, A.; Kamer, P. C. J.; van Leeuwen, P. W. N. M.; Goubitz, K.; Fraanje, J.; Veldman, N.; Spek, A. L. *Organometallics* **1996**, *15*, 835.

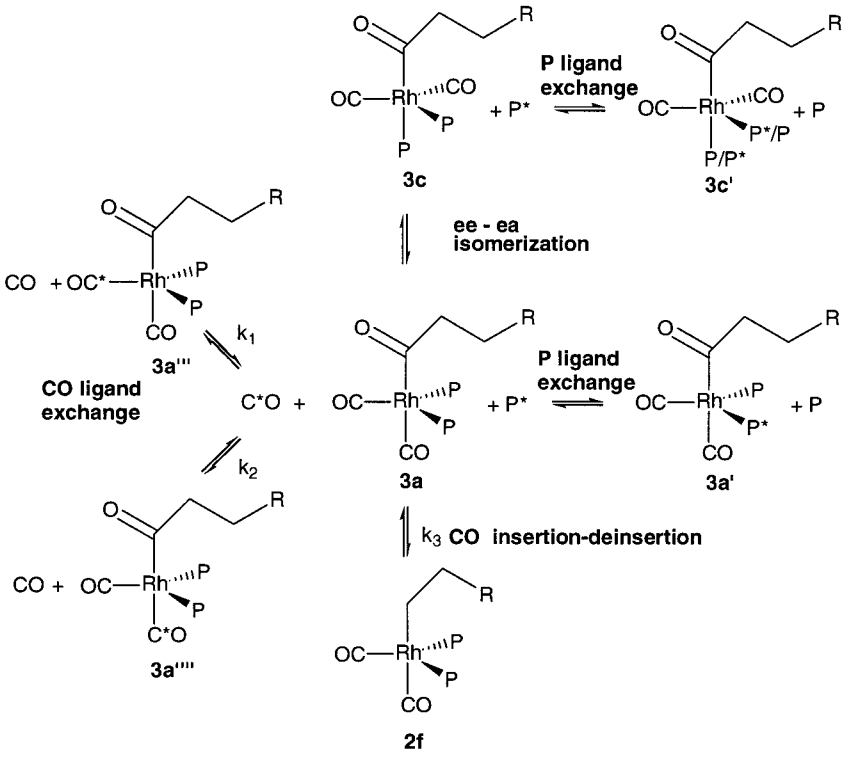

Figure 9. Different exchange processes of rhodium−acyl complexes.

rhodium−acyl complexes can have different reactivities toward hydrogen.

Exchange Processes Observed for the Rhodium−Acyl Complexes. The rhodium−acyl complexes **3a**−**d** are involved in several exchange processes, depending on the temperature. An overview of the exchange processes is presented in Figure 9. The complexes containing the branched aldehyde have been omitted for the sake of brevity. At room temperature one broad resonance for the free ligand is observed in the $^{31}P\{^{1}H\}$ NMR spectrum, indicating that there is an exchange with the coordinated ligand. A broad doublet at 109.5 ppm and a sharp resonance for the free ligand are observed when the temperature is decreased to 253 K. The exchange process of the coordinated and free ligands is slow on the NMR time scale at this temperature. One average resonance is observed for the two rhodium−acyl complexes with ee and ea coordinated phosphorus ligands. The isomerization between **3a,b** and **3c,d** is still fast on the NMR time scale. The phosphorus NMR broadens again upon cooling to 193 K, indicating that the isomerization becomes slow on the NMR time scale. In both complexes the phosphorus ligands lose their equivalence. Because of the low concentration of complex **3d** we were not able to resolve phosphorus coupling constants and chemical shifts of this complex. The ^{31}P NMR spectrum obtained at 193 K is shown in Figure 10. It should be noted that the free ligand shows fluxional behavior between two conformers. A variable-temperature ^{31}P NMR experiment of the free ligand at 173 K showed two different conformers in a 1:1 ratio (δ 65.7 and 64.7 ppm). The ^{31}P NMR spectrum 1a displayed in Figure 10 is a result of two different processes in which complex **3a** is involved. First, the two coordinated phosphorus atoms become magnetically inequivalent upon cooling (δ(P1) ∼112 ppm, δ(P2) ∼105 ppm). Second, interconversion between two ligand conformations becomes important; one of the phosphorus ligands is still in a fast exchange and the second phosphorus atom reaches the slow-exchange region. Simulation of these two processes results in the spectrum presented for spectrum 1b in Figure 10. Chemical shifts and coupling constants are presented in Table 7.

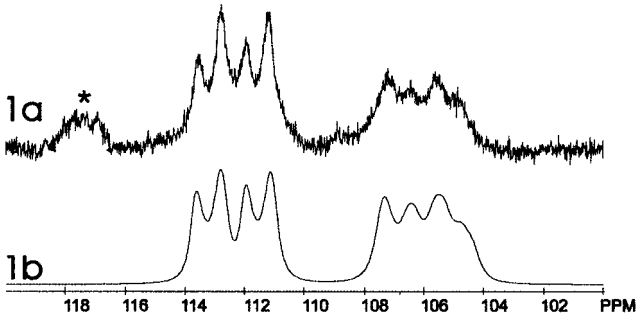

Figure 10. $^{31}P\{^{1}H\}$ NMR spectrum obtained after reaction of **2a**, 1-hexene, and CO at 193 K: (1a) experimental data; (1b) simulated $^{31}P\{^{1}H\}$ NMR spectrum of rhodium−acyl **3a** at 193 K, The resonance denoted by an asterisk belongs probably to the (minor) rhodium acyl **3d**.

Table 7. $^{31}P\{^{1}H\}$ NMR Data of 3a after Simulation of the Spectrum Obtained at 193 K

compd	$\delta(^{31}P)$ (ppm)	J_{PP} (Hz)	J_{RhP} (Hz)
isomer 1	P(1) 112.3	117	P(1) 202
	P(2) 105.8		P(2) 235
isomer 2	P(1) 112.4	115	P(1) 203
	P(2) 106.2		P(2) 222

The carbonyl ligands of complex **3a** are involved in several exchange processes at temperatures above 223 K. One averaged signal at δ 193 ppm for both carbonyl ligands and dissolved ^{13}CO was observed in the ^{13}C

NMR spectrum at room temperature, and one very broad resonance in the acyl region was observed. The averaged signal at 193 ppm is due to fast exchange of the carbonyl ligands with the dissolved ^{13}CO. The resonance of the equatorial CO is still very broad at 253 K (Figure 6, spectrum 1a), but the resonance of the apical CO sharpens. No resonance for the dissolved ^{13}CO gas was observed at this temperature. Simulation of the $^{13}C\{^1H\}$ NMR data (Figure 6, spectrum 1b) showed that the carbonyl ligands exchange with dissolved ^{13}CO gas with different rates (Figure 9). The pseudo-first-order rate constants obtained are $k_1 = 450$ s^{-1} and $k_2 = 25$ s^{-1}. The acyl group is involved in an insertion−deinsertion equilibrium ($k_3 = 25$ s^{-1}). The $^{13}C\{^1H\}$ NMR shows the immediate appearance of the acyl resonance of complex **3a** after bubbling ^{13}CO through a solution of the ^{12}CO rhodium−acyl complex at 253 K. This proves the presence of an insertion−deinsertion equilibrium. The rate of this insertion−deinsertion reaction (Figure 9, k_3) is much lower than the exchange rate of the equatorial carbonyl ligand with carbon monoxide in solution. Both the apical carbonyl and the rhodium−acyl resonances are well resolved at 233 K, indicating that exchange of both of these ligands with dissolved ^{13}CO is slow on the NMR time scale at this temperature (Figure 6, spectrum 2a, simulated spectrum 2b). The resonance of the equatorial carbonyl ligand is still very broad ($k_1 = 175$ s^{-1}). At 223 K (Figure 6, spectrum 3a), the exchange of the equatorial carbonyl ligand with dissolved ^{13}CO is also slow on the NMR time scale ($k_3 = 20$ s^{-1}) and a sharp resonance was observed for the equatorial carbonyl ligand together with a sharp resonance for dissolved ^{13}CO. The $^{13}C\{^1H\}$ NMR spectrum broadens again when the temperature was decreased further. This broadening is due to loss of equivalence of the phosphorus atoms. We were not able to resolve the different J_{CP} coupling constants of the inequivalent phosphorus atoms because the spectra remained broad upon cooling to 193 K.

Concluding Remarks

While both kinetics and in situ studies seem rather complicated at first sight, the system presents an ideal case to illustrate the basics of hydroformylation. The two most common types of kinetics are observed, and the effects of raising or lowering the concentration of any of the substrates leads to the result expected. In most ligand-modified rhodium systems the oxidative addition of H_2 plays no role in the kinetics. As shown previously,[25] the present ligands have high χ values—higher than those of most phosphites—and a relatively slow oxidative addition may indeed be expected. The rate-determining step of the hydroformylation reaction using this catalyst system cannot be attributed to one single step and is strongly dependent on the reaction conditions used. Therefore, the coordinatively saturated rhodium−hydride complex **2a** and the coordinatively saturated rhodium−acyl complexes **3a**−**d** are present in solution during the hydroformylation reaction, which was proven by in situ HP IR and HP NMR studies.

The deuterioformylation experiments showed that the rhodium−alkyl complex **2c** is irreversibly formed after alkene coordination and hydride migration. Therefore, we conclude that the regioselectivity for either the linear or the branched aldehyde is determined in these reaction steps.

In previous studies both we and others have discussed whether a bis-equatorial coordination mode of the phosphorus ligands should lead to high linear-to-branched ratios. The phosphorus diamide ligand used forms exclusively a hydride complex in which the phosphorus ligands are coordinated in the equatorial plane. The rhodium−acyl complexes observed contain phosphorus ligands coordinated in both the ee and ea coordination modes. As already argued by van der Veen and co-workers,[31] formation of a hydride complex having bis-equatorially coordinated phosphorus ligands does not guarantee a high linear-to-branched ratio in the product. As shown above, monodentate ligands may well have the flexibility to form ea complexes for the more hindered branched-alkyl and acyl complexes.

Experimental Section

General Information. All preparations were carried out under an atmosphere of argon using standard Schlenk techniques. All solvents were distilled from sodium. Ligand **1** was prepared according to literature procedures.[25] One-dimensional (high-pressure) NMR spectra (^1H, ^{31}P, and ^{13}C) were recorded on a Bruker DRX-300 spectrometer. The two-dimensional (high-pressure) NMR spectra were recorded on a Bruker AMX-200 spectrometer. The NMR flow cell experiments were recorded on a Bruker AM 200 WB spectrometer using a probe developed in Liverpool.[12] Chemical shifts are given in ppm referenced to TMS or H_3PO_4 (external). The in situ IR experiments were recorded on a Bio-Rad FTS-60A spectrophotometer. Every 1 s, seven IR spectra were recorded that were averaged to one spectrum. The IR spectra for the stoichiometric reactions were recorded on a Nicolet 510 FT-IR spectrometer.

Hydroformylation Experiments. These were performed in a stainless steel (SS 316) autoclave (196 mL). The autoclave is stirred mechanically and equipped with a reservoir, a pressure transducer, a thermocouple, and a sampling device. The autoclave is kept under constant pressure by a second pressurized stainless steel autoclave equipped with a reducing valve. In a typical experiment $Rh(acac)(CO)_2$ and ligand **1** were dissolved in 15 mL of toluene and introduced to the autoclave. After the autoclave was flushed with CO/H_2 (1/1), the autoclave was put under a pressure of 20 bar. The autoclave was heated to 41 °C, and after 2 h the substrate solution was charged into the reservoir and added to the reaction mixture by overpressure. The alkene was filtered over neutral alumina to remove peroxides. During the reaction, several samples were taken and immediately quenched by adding an excess of $P(O\text{-}n\text{-}Bu)_3$, to deactivate hydroformylation or isomerization active rhodium species. The samples were analyzed by GC using decane as internal standard. In a typical deuterioformylation experiments, 10 mg (3.8 μmol) of $Rh(acac)(CO)_2$ and 10 equiv of ligand **1** were dissolved in 15 mL of toluene and introduced to the autoclave. The autoclave was pressurized with 15 bar of CO/D_2 (1/2). The autoclave was heated to 41 °C, and after 2 h the substrate solution was charged into the reservoir and added to the reaction mixture by overpressure of CO. The alkene was filtered over neutral alumina to remove peroxides. The autoclave was pressurized up to 20 bar using CO. During the reaction several samples were taken and quenched immediately by adding an excess of $P(O\text{-}n\text{-}Bu)_3$, to deactivate hydroformylation- or isomerization-active rhodium species. The samples were analyzed by GC using decane as internal standard. The deuterium contents in the substrate and products during the reaction were determined using gas

chromatography/mass spectrometry. After 2 h, complete conversion was reached and the reaction mixture was quenched with $P(O\text{-}n\text{-}Bu)_3$. The aldehydes were distilled off and further purified by column chromatography on silica gel. As eluent pentane was used to remove toluene and decane from the sample (R_f(aldehydes) = 0), dichloromethane was used to recover the mixture of linear and branched aldehydes (R_f(aldehydes) = 1). ^1H and ^2H NMR data of the aldehydes were identical with the data obtained by Casey et al.[29]

High-Pressure FT IR Experiments. These were performed in a stainless steel (SS 316) 50 mL autoclave equipped with IRTRAN windows (ZnS, transparent up to 700 cm^{-1}, 10 mm i.d., optical path length 0.4 mm), a mechanical stirrer, a temperature controller, and a pressure transducer. In a typical experiment 10 mg (0.039 mmol) of $Rh(acac)(CO)_2$ and 114 mg (0.39 mmol) of ligand **1** were dissolved in 15 mL of cyclohexane. The yellow solution was introduced to the autoclave and put under a pressure of 15 bar of CO/H_2 (1/1). Complete conversion to $HRhL_2(CO)_2$ (**2a**) is reached after 1 h of heating at 80 °C or 2 h of heating at 40 °C. For the stoichiometric reactions, after complete conversion to the hydride complex, the autoclave was cooled to room temperature. After depressurization the autoclave was flushed with CO to remove the H_2, and 1.0 mL (6.4 mmol) of 1-octene was added slowly. The autoclave is put under a pressure of 5 bar of CO, and the IR spectra were recorded at room temperature. Finally 10 bar of H_2 was added, and the reaction was followed using IR spectroscopy. In the in situ IR experiments the autoclave is equipped with an extra reservoir. A 0.5 mL (3.2 mmol) amount of 1-octene was added by overpressure. The IR spectra were recorded at 40 °C. Recording was started several seconds before the alkene was added.

High-Pressure NMR Experiments. In a typical NMR tube experiment, 20 mg (0.079 mmol) of $Rh(acac)(CO)_2$ and 114 mg (0.39 mmol) of ligand **1** were dissolved in 2.0 mL of toluene-d_8. The yellow solution was introduced to an argon-flushed (10 mm) sapphire HP NMR tube[31] and put under a pressure of 15 bar of CO/H_2 (1/1). Complete conversion to **2a** was reached after 1 h of heating at 80 °C, and the NMR tube was depressurized. CO was bubbled through the solution, and 0.3 mL (2.4 mmol) of 1-hexene was added. The pale yellow solution becomes bright yellow when 1-hexene is added. The HP tube was pressurized with 3 bar of CO, and the NMR spectra were recorded. A 10 mm thick-walled glass tube instead of the sapphire HP tube[31] was used for the two-dimensional NMR experiments to obtain better resolution. In a typical NMR flow cell[12] experiment, 20 mg (0.079 mmol) of $Rh(acac)(CO)_2$ and 114 mg (0.39 mmol) of ligand **1** were dissolved in 5 mL of toluene-d_8. The cell was pressurized to 20 bar of CO/H_2 (1/2). The sample was cooled to room temperature after 1 h of heating at 80 °C. 1-Hexene was injected at −20 °C, and the NMR spectra were recorded. Simulations of the carbon and phosphorus NMR data were performed using gNMR V4.1.0.

OM000785H